Journal of Organometallic Chemistry, 331 (1987) 207–219
Elsevier Sequoia S.A., Lausanne – Printed in The Netherlands

The seven-coordinate hydrido-tantalum complexes $[Ta(H)(CO)_{6-n}(oligophos)]$: preparation and dynamics

Dieter Rehder *, **Michael Fornalczy and Peter Oltmanns**
Institut für Anorganische Chemie der Universität, D-2 Hamburg 13 (F.R.G.)

(Received February 25th, 1987)

Abstract

The hydrido complexes *cis*-$[HTa(CO)_4P_2]$ ($P_2 = Ph_2PCH_2CH_2PPh_2$), $HTa(CO)_3P_m$ ($P_m = P_3$: $PhP(CH_2CH_2PPh_2)_2$, P_4: $[Ph_2PCH_2CH_2PPhCH_2]_2$, PP_3: $P(CH_2CH_2PPh_2)_3$) have been obtained from the photo-chemically produced complexes $[Et_4N][Ta(CO)_4P_m]$ by ion-exchange chromatography on silica gel. The anionic and neutral complexes have been characterized by IR and ^{31}P and ^1H NMR spectroscopy. The temperature-dependent ^1H(hydride)–^{31}P NMR coupling patterns are interpreted in terms of a hydride-capped octahedral structure with restricted migration of the H^- ligand between the octahedral faces.

Introduction

Hepta-coordinated hydridocarbonyl complexes of the group 5 metals, stabilized by di- to tetra-dentate phosphines, are suitable reagents for the transfer of hydrogen to organic substrates; eq. 1 and 2 [1,2].

$$HV(CO)_4dppm + CH_2{=}C(Me)CH{=}CH_2 \rightarrow \eta^3\text{-}\{C_3H_3Me_2\}V(CO)_3dppm \qquad (1)$$

($dppm = Ph_2PCH_2PPh_2$)

$HV(CO)_4P_2$ + 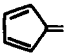 $=CMe_2 \rightarrow \eta^5\text{-}\{C_5H_4CHMe_2\}V(CO)_2P_2$ (2)

The interaction of isoprene (eq. 1) with $HV(CO)_4P_2$ ($P_2 = Ph_2PCH_2CH_2PPh_2$) gives the neutral 17-electron species $V(CO)_4P_2$ [1], which is also formed by thermal decomposition of $HV(CO)_4P_2$ [3] or by oxidation of $[Et_4N][V(CO)_4P_2]$ with $[C_7H_7][BF_4]$ [4–6]. On the other hand, the metal–hydrogen bond appears to be essentially stable towards UV-irradiation: The complexes $HM(CO)_4P_m$ ($P_m = P_2$, P_3; M = V, Nb) are converted to $HM(CO)_2(P_m)_2$ [7]. The conversion of carbonylvanadates and hydridocarbonylvanadium complexes into phosphine derivatives of $V(CO)_6$ under suitable reaction conditions presents an interesting possibility for the synthesis of the still unknown Nb and Ta homologues, the search for which is continuing [8].

0022-328X/87/$03.50 © 1987 Elsevier Sequoia S.A.

In earlier work we studied the chemistry of phosphine-stabilized carbonyl and carbonylhydrido complexes of V [7,9,10] and Nb [7,11], and we now report on new results for the tantalum analogues. The hydrido complexes exhibit fluctionality, and the analysis of the NMR spectra allows determination of some interesting features of the structure in solution. To our knowledge, only three carbonyltantalates ($[Ta(CO)_5PPh_3]^-$, $[Ta(CO)_4P_2]^-$ [12], $[Ta(CO)_4P_3]^-$ [7]) and only two hydrido species belonging to the $HM(CO)_nP_m$ category ($HTa(CO)_3P_3$ [7], $HTa(CO)_2(dmpe)_2$, dpme = $Me_2PCH_2CH_2PMe_2$ [13]) have been described previously.

Results and discussion

Preparation and IR characteristics

The carbonyltantalates(−I) are obtained by UV irradiation of $[Et_4N][Ta(CO)_6]/P_m$ 1/1 in THF. Monitoring by IR spectroscopy reveals intermediate formation of the pentacarbonyltantalates $[Ta(CO)_5P_m]^-$, shown by the intermediate appearance of a sharp $\nu(CO)$ at 1987 cm^{-1} (A_1(CO-*cis*); local C_{4v} symmetry). The final products are the red complexes *cis*-$[Et_4N][Ta(CO)_4P_m]$, which have IR spectra characteristic of the group 5 tetracarbonylmetalates(−I) (local symmetry: C_{2v}), i.e. a strong, sharp $\nu(CO)$ at ca. 1900 cm^{-1} (A_1(CO-*cis*)), and a poorly resolved system of 3 bands between ca. 1800 and 1750 cm^{-1} (A_1(CO-*trans*), B_1, B_2; cf. Table 1).

Trisubstitution does not occur with the potentially tri- and four-dentate ligands P_3, P_4 and PP_3. In the case of the corresponding vanadium compounds, the tricarbonyl species is readily formed [10]; the tendency for replacement of a third carbonyl in the niobium complexes, although it can be achieved [7], is markedly less pronounced than in the vanadium system.

On silica gel, the tetraethylammonium cation is exchanged for the H^+ of the potentially acidic silanol groups of the gel. The hydrido complex thus formed is removed from the equilibrium by elution with THF. In the case of P_3, P_4 and PP_3, the complexes are further stabilized by removal of one CO and concomittant formation of bicyclic, five-membered chelate structures. For P_3 and PP_3, this process takes several hours, and the tetracarbonyl species can be detected by IR (see Fig. 1)

Table 1

CO stretching frequencies (cm^{-1}), Nujol mulls

$[Ta(CO)_4P_2]^-$ [a]	1900w	1795vs	1750sh	
$[Ta(CO)_4P_3]^-$ [b]	1898m	1790s	1780sh	1745sh
$[Ta(CO)_4P_4]^-$	1898w	1780vs	1750sh	
$[Ta(CO)_4PP_3]^-$	1880w	1785vs	1755sh	1725sh
$HTa(CO)_4P_2$	1990m	1865vs,br		
$HTa(CO)_4P_3$	1992m	1860vs		
$HTa(CO)_4P_4$	1990m	1855vs	1885sh	
$HTa(CO)_3P_3$ [b]	1935m	1810s		
$HTa(CO)_3P_4$	1925m	1800s		
$HTa(CO)_3PP_3$	1930m	1805s		
$HTa(CO)_2(P_2)_2$	1765			

[a] Compare ref. 12: 1908s, 1800vs, 1779s and 1752m. [b] From ref. 7.

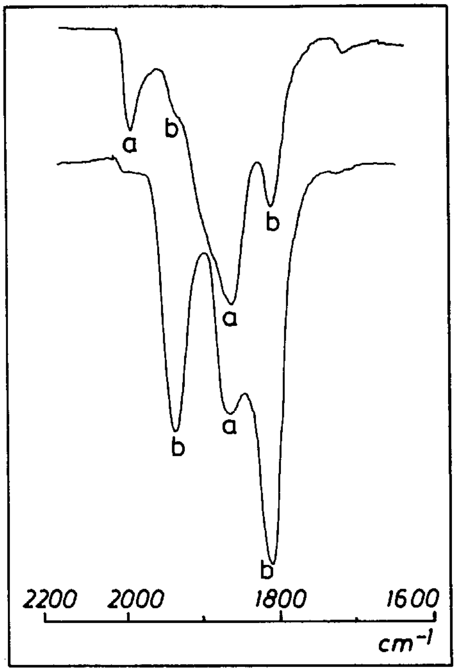

Fig. 1. CO stretching region of $HTa(CO)_nP_3$ (THF solution), showing the development from $n = 4$ (a) to $n = 3$ (b). The time between the two spectra was 5 days during which the solutions were kept at 258 K.

and ^1H NMR spectroscopy. The complex $HTa(CO)_4P_2$, in contrast to the labile $HNb(CO)_4P_2$ [11], can be stored at 0 °C for several weeks without decomposition; but it is less stable than $HV(CO)_4P_2$ [7,14]. Irradiation of *cis*-[$HTa(CO)_4P_2$] in THF yields *trans*-[$HTa(CO)_2(P_2)_2$]. The *trans*-configuration is evident from the single CO stretching mode, and is consistent with that found in *trans*-[$HTa(CO)_2(dmpe)_2$] [13] and *trans*-[$HMo(CO)_2(diphos)_2$]$^+$ [15]. The overall reaction scheme is shown in Scheme 1. Yields are around 80%; in each case a small amount of the hydrido complex decomposes on the chromatographic column to form $[Ta(CO)_6]^-$. Our mild method for preparation of $HM(CO)_nP_m$ species is more convenient (particularly in that it leads to considerably higher yields of pure products) than the action of H_3O^+

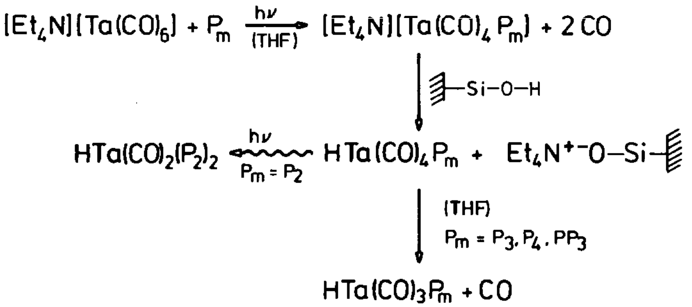

Scheme 1

on the carbonyl metalates used for the preparation of $HV(CO)_4P_2$ [6], or the high pressure synthesis reported for $HTa(CO)_2(dpme)_2$ [16].

IR data are listed in Table 1. Except for $HTa(CO)_4P_2$ and $HTa(CO)_2(P_2)_2$, they do not permit configurational assignment, i.e. distinction between meridional and facial configuration of the $Ta(CO)_3P_m$ core. The comparatively broad bands (cf. Fig. 1) probably obscure several overlapping components belonging to positional isomers created by the migrating hydride ligand (see the discussion of the ^1H NMR spectra below).

^{31}P NMR spectra

In contrast to the ^{31}P NMR spectra of the V and some of the Nb complexes, which give broad, unresolved signals due to coupling of the nucleus ^{31}P with ^{51}V (nuclear spin $I = 7/2$, electric nuclear quadrupole moment $Q = -0.05 \times 10^{-28}$ m^2) and with ^{93}Nb ($I = 9/2$, $Q = -0.2 \times 10^{-28}$ m^2), those of the Ta complexes are well resolved and can be employed in the discussion of the structure. The sharp signals are a consequence of effective relaxation decoupling between the nuclei ^{31}P and ^{181}Ta, which possesses the extremely large Q value of 3×10^{-28} m^2 ($I = 7/2$).

The shift and coupling data are summarized in Table 2, and representative spectra ($[Ta(CO)_4PP_3]^-$ and $HTa(CO)_3P_3$) are shown in Figs. 2 and 3. The following labeling scheme (cf. also Scheme 2) will be used throughout: uncoordinated phosphorus functions, X; coordinated phosphorus functions, A (for PPh_2), B (for PPh) and C (for P). An asterisk indicates inequivalence intrinsic to the coordinated

Table 2

$^{31}P\{^1H\}$ NMR data [a]

Complex [b]	PPh_2 (A)	PPh (B)	P (C)	X [c]	Spin system [d]
$[Ta(CO)_4P_2]^-$	46.8				A_2X
$[Ta(CO)_4P_3]^-$	48.2(d: 22)	48.7(dd: 37, 22) [e]		−14.2(d: 37)	ABX
$[Ta(CO)_4P_4]^-$ [f]	47.9(m) [f]			−11.8(m)	ABXX*
$[Ta(CO)_4PP_3]^-$	50.3(d: 21)		48.3(dt: 21, 31) [g]	−10.6(d: 31)	ACX_2
$HTa(CO)_4P_2$	43.3				A_2
$HTa(CO)_3P_3$ [h]	45.2(d: 1.9)	72.7(t: 1.9)			A_2B
$HTa(CO)_3P_4$ [h]	70.5(d: 3.6)	46.9(dd: 7.8, 3.7) 45.9(dd: 7.6, 3.8)		−14.2 [i]	ABB*X
$HTa(CO)_3PP_3$ [h]	50.2		72.2(d: 30) [j]	14.7(d: 32)	A_2CX
$HTa(CO)_2(P_2)_2$	44.2, 64.1				$A_2A'_2$ [k]

[a] At room temperature or (footnote *h*) 305 K. Chemical shifts (ppm) relative to H_3PO_4, and coupling constants (Hz) (in parentheses: d = doublet, t = triplet, q = quintet, dd = doublet of doublets, ddd = doublet of doublets of doublets, dt = doublet of triplets (triplet splitting < doublet splitting), td = triplet of doublets (triplet splitting > doublet splitting), tt = triplet of triplets, m = poorly resolved or undecoded multiplet; singlet if not indicated). [b] Abbreviations: $P_2 = Ph_2PCH_2CH_2PPh_2$, $P_3 = PhP(CH_2CH_2PPh_2)_2$, $P_4 = (Ph_2PCH_2CH_2PPhCH_2)_2$, $PP_3 = P(CH_2CH_2PPh_2)_3$. [c] Uncoordinated phosphorus function. [d] See text and Scheme 2 for the labeling system. [e] The larger coupling constant is J(BX). [f] A + B. Only one signal is observed, possibly representing two isomers; cf. Scheme 2. [g] The smaller coupling constant is J(AC), the larger J(AX). [h] At 305 K. [i] Unresolved. At 220 K: −16.3 (d: 4.0). [j] Only the coupling to the uncoordinated PPh_2 (J(CX)) is observed. [k] The inequivalence of the two sets of PPh_2 groups is created by the hydride ligand; cf. Scheme 3, (b).

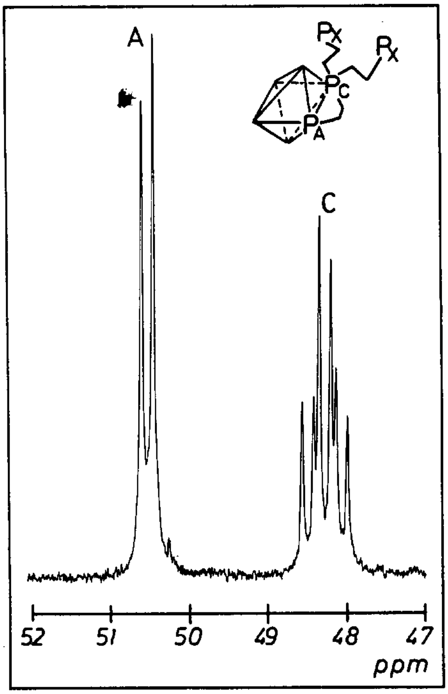

Fig. 2. 145.8 MHz $^{31}P\{^1H\}$ NMR spectrum of a THF solution of $[Et_4N][Ta(CO)_4PP_3]$ at room temperature (region for coordinated P atoms only).

phosphine ligand (e.g. B and B★), and a dash inequivalence created by the H^- (Y in the labeling system) ligand (e.g. A and A′).

The spectra of the four anions are consistent with chelate-5 ring structures, as shown in Scheme 2. In the ^{31}P NMR spectra of the hydrido complexes, the $^{31}P-^{31}P$ coupling constants between coordinated P-atoms are rather small throughout compared with those of the parent anionic carbonyl complexes. It is possible that in the hydrido complexes, the three-bond coupling between coordinated P-atoms along the carbon back-bone is partially cancelled out by two-bond coupling of opposite sign via the metal centre. This is especially pronounced in $HTa(CO)_2(P_2)_2$, where coupling is below the limit of resolution (< 0.5 Hz). The two singlets observed in the spectrum of this compound belong to two inequivalent sets of PPh_2 groups, created by restricted mobility of H^- (see next section). The same phenomenon is observed for $HTa(CO)_3P_3$ below 220 K (Fig. 3). The equally small $J(B^\star X)$ and $J(BA)$ in $HTa(CO)_3P_4$ (3.7 Hz) suggest an arm-on/arm-off fluctionality of the PPh_2 functions A and X.

^1H NMR spectra (hydride region)

Shift values and $^1H-^{31}P$ coupling constants are listed in Table 3. For comparison, data for selected vanadium and niobium complexes are included.

A straightforward interpretation of the spectra can be made by assuming that the CO and P ligands are arranged in an octahedral array, with the hydride ligand capping octahedral faces [7,10,11,15]. For crystalline $HTa(CO)_2(dpme)_2$, this struc-

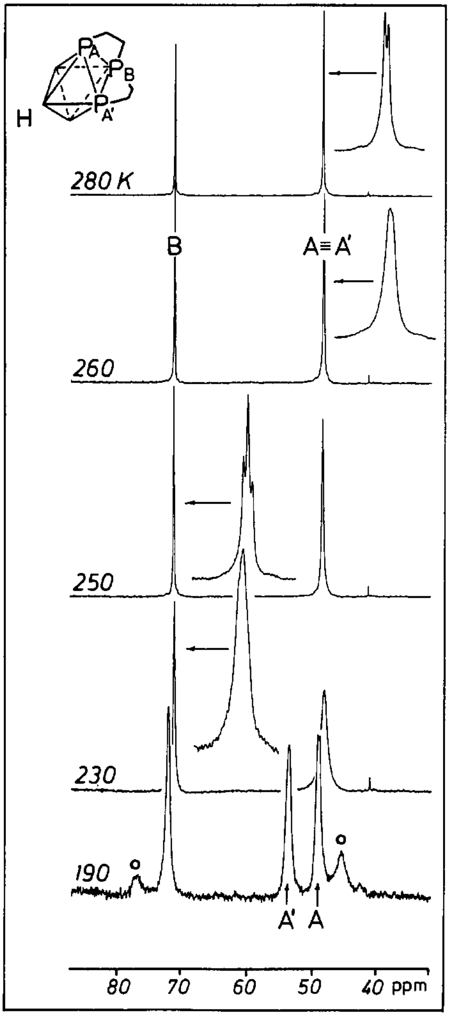

Fig. 3. Variable temperature 32.4 MHz $^{31}P\{^1H\}$ NMR spectra of a THF solution of $HTa(CO)_3P_3$. The expansion factor for the expanded signals in the four upper spectra is 30. The two signals marked "O" in the 190 K spectrum are possibly from $HTa(CO)_4P_3$ impurity.

ture has been verified by X-ray diffraction [13]. For $HV(CO)_4P_2$, an X-ray study revealed a distorted pentagonal-bipyramidal arrangement with H^- located in the pentagonal plane between P and CO [17], but in the solution the structure appears to be that of a face-capped octahedron [10a]. The ^1H and ^{31}P NMR patterns of $[HMo(CO)_2(diphos)_2]^+$ [15] and $HTa(CO)_2(dmpe)_2$ [13] have been approximated on the basis of this model to computed spectra for mixtures of non-pairwise (Scheme 3, (a)) exchange or (diphos = P_2) almost exclusive pair-wise exchange (b) of the phosphorus positions. This latter case is illustrated in Scheme 3 in two equivalent views: (i) exchange of the two sets, A and A', of phosphorus atoms, and (ii) the exchange of H^- positions (dashed faces). In addition, ^{13}CO NMR spectra of $[Mo(CO)_2(diphos)_2]^+$ have revealed migration of H^- between equivalent faces

(Continued on p. 215)

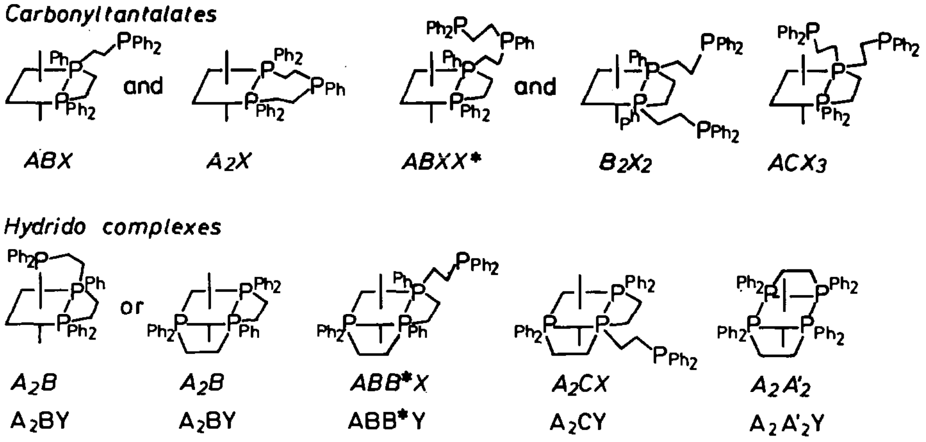

A, B, C = coordinated PPh2 (A), PPh (B), P(C); X = uncoordinated phosphorus

Y = H⁻

Scheme 2

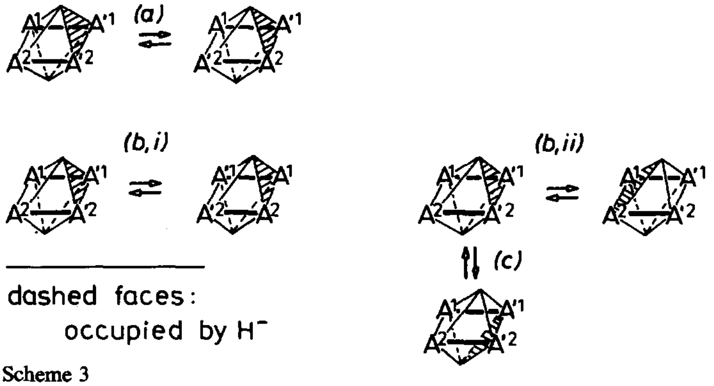

dashed faces:
occupied by H⁻

Scheme 3

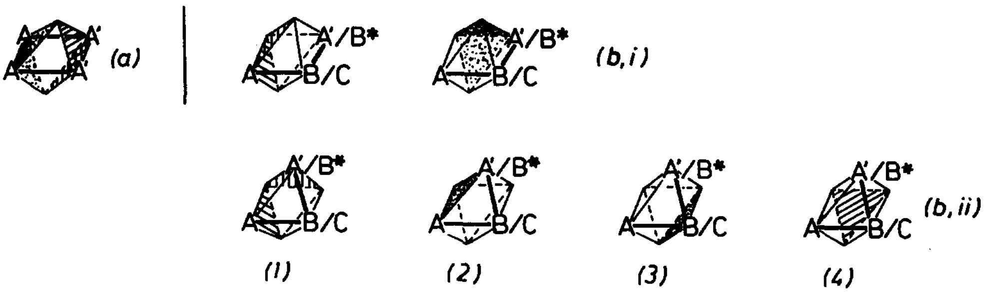

Scheme 4

Table 3

^1H (hydride) NMR data for hydridotantalum and some related niobium and vanadium complexes

Complex	Temperature (K)	Spin system[c]	δ (J(H–P))[b]	Temperature (K)	Spin system[c]	δ (J(H–P))[b]
cis-[$HM(CO)_4P_2$]						
M = Ta	290	A_2Y	−3.38(t: 21)	185		−3.6[d]
M = Nb[e]	295	A_2Y	−3.80(t: 18)			
M = V[f]	295	A_2Y	−5.03(t: 26)			
$HM(CO)_3P_3$						
M = Ta[g]	300	A_2BY	−2.33(td: 37, 18)[h]	220	A_2Y; A_2BY	−2.36(t: 39); −2.57("t"[i]: 39)
M = Nb[e]	297	A_2BY	−2.94(td: 31, 12)[h]	190	AY; A′Y	−2.21(d: 22); −2.75(d: 22)
M = V[j]	295	A_2BY	−4.54(td: 39, 20)[h]			
$HTa(CO)_3P_4$	323	ABB^*Y	−2.48(ddd: 42, 36, 14)[k]	190	AY; B^*Y	−2.53(d: 54); −2.80(d: 54)[k]
$HTa(CO)_3PP_3$	300	A_2CY	−2.38(td: 36, 16)[h]	190		−2.4[l]
trans-[$HTa(CO)_2(P_2)_2$]	297	$A_2A'_2Y$	−3.24(tt: 96, 17)[m]	210		−3.53("tt"[l])
trans-[$HM(CO)_2P_4$]						
M = Nb[g]	300	A_2B_2Y	−1.33("tt"[l]: 11.5)[n]			
M = V[j]	295	A_2B_2Y	−3.62(tt: 113, 18)[m]			
trans-[$HTa(CO)_2(dmpe)_2$][o]	370	A_4Y	[p](q: 52)	281	$A_2A'_2Y$	−4.17(tt: 89, 14)

[a] For abbreviations of the phosphine ligands see Table 2, footnote *b*; dmpe = $Me_2PCH_2CH_2PMe_2$. [b] For abbreviations of the spectral patterns see Table 1, footnote *a*. [c] For the labeling of the spin systems see text and Schemes 2–4; Y is the hydride ligand. [d] Very broad, unresolved resonance. [e] From ref. 11. [f] From ref. 14. [g] From ref. 7. [h] The larger (triplet) coupling is *J*(YA). [i] See text for discussion. [j] From ref. 10a. [k] Cf. Fig. 4. [l] Poorly resolved. [m] The larger triplet coupling is *J*(YA). [n] Only the YA coupling is resolved. [o] From ref. 13. [p] Not reported.

above and below the P_4 plane ((c) in Scheme 3) [15], possibly via a transitory pentagonal-bipyramidal state with the hydride located between CO and P, as is seen in the "frozen-in state", i.e. solid state structure, of $HV(CO)_4P_2$ [17].

We shall discuss the ^1H NMR spectra of the complexes $HTa(CO)_nP_m$ in terms of the possibilities for, and limitations on, the migration of the hydride ligand.

The first constraint to an essentially free motion of the hydride ligand arises from the fact that faces which are edge-spanned by the ethylene back-bone of the oligodentate phosphine ligand are partly hidden, and hence are unfavourable sites which are not occupied by the hydride. In *trans*-$[HTa(CO)_2(P_2)_2]$, 4 faces (Scheme 4, (a)) remain to be capped by H^-. At room temperature, H^- cannot surmount the barrier built up by the carbon back-bones, and hence there is no way for the hydride ligand to move between the two sets of faces (Scheme 4, (a), dotted and striped areas, respectively). As a consequence, the four PPh_2 groups fall within two sets of inequivalent P centres (A and A′), giving rise to a triplet of triplet in the ^1H NMR with a large $^1H-^{31}P$ coupling of 96 Hz for the P atoms in the immediate proximity of H^-, and a small coupling constant of 17 Hz for the two more distant ones. The two J values mark the two extremes to be expected for $^1H-^{31}P$ coupling in hydridophosphinetantalum complexes. As has been shown for $HTa(CO)_2(dmpe)_2$, the four P atoms are equilibrated with respect to H^- at elevated temperatures (cf. Table 2).

There are six allowed positions for H^- in *cis*-$[HTa(CO)_4P_2]$, and there are no ethylene barriers preventing the H^- from migrating liberately between all six faces. Of these, only two allow each of the P atoms to come close to H^-; hence the resulting relatively small coupling constant of 21 Hz.

The situation is more complex for the tricarbonyl species. We shall first consider the ^1H NMR patterns of $HTa(CO)_3P_3$ and $HTa(CO)_3PP_3$. In the facial configuration there are five, and in the meridional four, possible occupational sites for H^- (Scheme 4, (b)). In either arrangement, the terminal PPh_2 functions are equilibrated ($A \equiv A'$) by the migrating H^-. There is no position in which H^- comes close to the bridgehead phosphorus, and this is reflected in the small $J(H-P_B)$ and $J(H-P_C)$ values, which are very close to the lower limits found in $HTa(CO)_2(P_2)_2$. The medium values of the coupling constants $J(H-P_A)$, 37 Hz, reflect the fact that, on an average, P(A) and P(A′) are further from H^- than in $HTa(CO)_2(P_2)_2$ (see also the more detailed description below). The resulting spin system at room temperature is $A_2B(C)Y$ for the facial and meridional configurations. As the temperature is lowered to 220 K, two triplets with slightly different shift values but similar coupling constants arise (cf. also ref. 7). The inequivalence of the two triplets, which indicate that exchange between different isomers is drastically slowed down, is also demonstrated by the fact that the triplet at high field broadens more quickly as the temperature is further decreased.

Owing to the inequivalence of the two coordinated PPh functions B and B*, the ^1H NMR spectrum of $HTa(CO)_3P_4$ (Fig. 4) is a doublet of doublets of doublets with two comparatively large coupling constants (42 and 36 Hz: $J(H-P_A)$ and $J(H-P_{B^*})$; cf. Scheme 4, (b)) and a small $J(H-P_B)$ 14 Hz. Again, distinction between meridional and facial ligand arrangement cannot be made on the basis of the room temperature spectra.

At low temperature, a four-line pattern arises (Fig. 4), very reminiscent of the corresponding ^1H NMR spectrum of $HNb(CO)_3P_3$ [11], but clearly different from

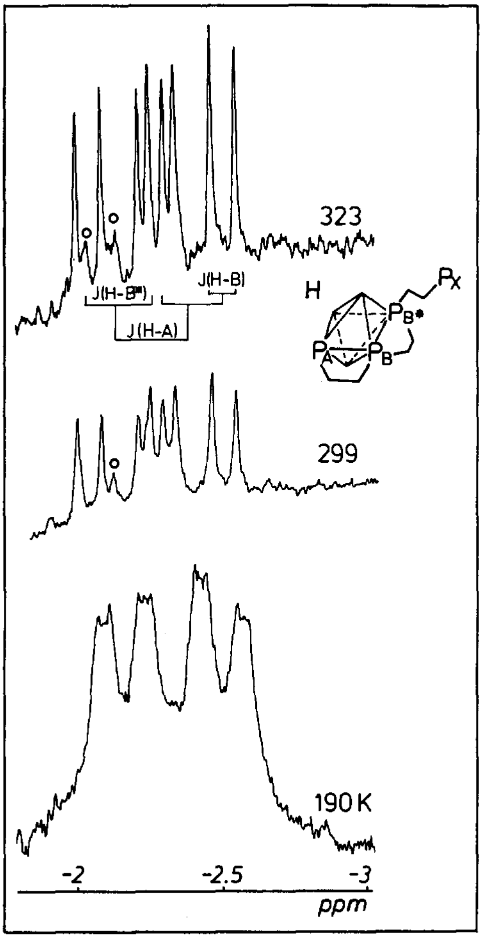

Fig. 4. Variable temperature 80 MHz ^{1}H NMR spectra (hydride region) of HTa(CO)$_3$P$_4$ in THF-d_8. Signals from a small impurity (O) are not assigned.

that of HTa(CO)$_3$P$_3$. The four lines result from two overlapping doublets exhibiting J(H–P$_A$) and J(H–P$_{B\star}$) in the case of HTa(CO)$_3$P$_4$, and J(H–P$_A$) and J(H–P$_{A'}$) in the case of HNb(CO)$_3$P$_3$. The small coupling J(H–P$_B$) is not resolved. Although, in HTa(CO)$_3$P$_4$, the inequivalency of P(A) and P(B*) is intrinsic to the coordinated phosphine, a second, even more important component which increases this inequivalence has to be considered. This has been shown to be the case for HM(CO)$_3$P$_3$ (Fig. 3), where two ^{31}P NMR signals in the low-temperature spectrum indicate that P(A) and P(A′) are in fact inequivalent as a consequence of frozen-in positional (H$^-$) isomers.

In the meridional arrangement, the two sets of four isomers (with A and A′/B* mutually next to H$^-$ as indicated by the striped and dotted areas, respectively; see (b, i) in Scheme 4) correspond to two distinguishable PPh$_2$ groups A and A′ and thus two doublets if exchange between the two sets is slow on the NMR time scale. For the facial arrangement, the five positional isomers fall into four non-equivalent sets (Scheme 4, (b, ii)): 2 isomers with A or A′/B* (1), 1 isomer with A and A′/B* in the vicinity of H^- (2); 1 isomer with B close to H^- (and A and A′/B* far off) (3); 1 isomer where none of the three P atoms comes close to H^- (4). Only (1) and (2) can give rise to a doublet splitting, and three doublets should arise, and since this is not observed the facial configuration for $HTa(CO)_3P_4$ seems to be excluded.

On the other hand, facial configuration may be possible for $HTa(CO)_3P_3$ if it is assumed that there is still some mobility for H^- left at ca. 220 K. In this case, one of the two triplets observed at 220 K can be generated by (2) (or a mixture of (1) and (2)), and the other, a broader one, actually a triplet of doublets with non-resolved doublet splitting, by mixing of the sets (1) and (3). The ^{31}P NMR spectrum at 220 shows that A and A′ are still averaged by H^- migration: Only one singlet is observed at this temperature, in contrast to the behaviour of $HNb(CO)_3P_3$, which at 220 K shows two distinct signals for A and A′ [11]. At 190 K, the inequivalence of A and A′ is also evident for $HTa(CO)_3P_3$ (Fig. 3); at this temperature, however, the ^1H resonance is a broad, unresolved band.

Conclusion

We have shown that the solution structures of the complexes $HTa(CO)_nP_m$ ($n + m = 6$; m = number of coordinating P atoms) can be interpreted as monocapped octahedra with the hydride ligand capping those octahedral faces which are not edge-spanned by an ethylene back-bone of the phosphine ligand. For $n = 4$ ($P_m = P_2$) and 3 ($P_m = P_3$, P_4, PP_3), there are six ($n = 4$), five ($n = 3$, facial configuration) and four ($n = 3$, meridional configuration) faces available for H^-, and at room temperature these faces are equally occupied and rapid site exchange occurs. This is still so at temperatures of ca. 200 K for $HTa(CO)_4P_2$, but in the tricarbonyl species, the structures become partly rigid. The spectra in the low temperature range allow tentative configurational assignments, namely facial for $HTa(CO)_3P_3$ (with some residual migration of H^-) and meridional for $HTa(CO)_3P_4$ and possibly also for $HTa(CO)_3PP_3$. The meridional configuration appears also to be achieved in $HNb(CO)_3P_3$. These assignments are supported by the ^{31}P NMR spectra at 220 K, which show a single resonance for the two PPh_2 groups in the case of $HTa(CO)_3P_3$ and two resonances in the case of $HNb(CO)_3P_3$, indicative of two PPh_2 groups distinguished by the position of H^-. The situation revealed by the low temperature ^1H and ^{31}P NMR spectra of $HM(CO)_3P_3$ is comparable to that of *trans*-$[HTa(CO)_2(P_2)_2]$ at room temperature, where the exchange between the four available H^- sites is subject to constraints imposed by the carbon back-bones (creating two inequivalent PPh_2 sets), and is restricted to the motion of H^- between the two sets of faces above and below the P_4 plane.

Experimental

General

Starting materials: $Na[Ta(CO)_6]$ was prepared by reductive carbonylation of $TaCl_5$ under pressure as described by Calderazzo et al. [18]. The ether solution of this compound was stabilized by addition of diglyme, the ether removed in vacuo, and the residue cooled to 253 K and treated with a solution of $[Et_4N]Br$ in ethanol. $[Et_4N][Ta(CO)_6]$, a yellow powder, was precipitated from this solution by addition of water and dried thoroughly before use. Silica gel (kieselgel 60, 70–230 mesh ASTM; Merck) was activated for 2 h in high vacuum, treated with N_2, and suspended in THF. Phosphines were purchased (Strem). All operations were carried out under N_2 and in oxygen-free anhydrous solvents of analytical quality. Irradiations were carried out in a 100 ml DEMA irradiation apparatus (Mangels, Bonn), equipped with a water-cooled quartz immersion well for the high pressure mercury lamp (HPK 125, Philips). During irradiation, a weak N_2 stream was passed through the solution via a sintered disc at the bottom of the reaction vessel.

Spectra. IR: Perkin–Elmer 577 spectrometer, ca. 0.02 *M* THF solutions in 0.1 mm KBr cuvettes. ^{1}H NMR: Bruker spectrometers WP 80 and AC 100, THF d_8, 5 mm diameter vials, standard: TMS, $^{31}P\{^1H\}$ NMR: 32.4 MHz (Bruker WP 80) and ($[Ta(CO)_4P_m]^-$; $P_m = P_3, P_4, PP_3$) 145.8 MHz (Bruker AM 360), THF/THF-d_8 1/2 in 10 mm vials, standard: 80% H_3PO_4.

Preparation of complexes

cis-$[(C_2H_5)_4N][Ta(CO)_4P\{CH_2CH_2P(C_6H_5)_2\}_3]$: A solution of 550 mg (1.15 mmol) of $[Et_4N][Ta(CO)_6]$ and 771 mg (1.15 mmol) of the phosphine PP_3 in 100 ml THF was irradiated for 45 min, during which the colour changed from yellow to deep-red. The solution was concentrated to 20 ml (vacuum, room temperature) and 20 ml of n-pentane was added with vigorous stirring. A viscous, orange-red oil precipitated out and after decantation of the essentially colourless supernatant solution, was washed with 5 ml of pentane and dried under high vacuum for 3 h to yield a dark red powder. Yield 850 mg (0.78 mmol) = 68%.

The other anionic complexes were prepared similarly: *cis*-$[(C_2H_5)_4N][Ta(CO)_4(C_6H_5)_2PCH_2CH_2P(C_6H_5)_2]$ (irradiation time 1.7 h; yield 84%; red powder, which precipitates out during concentration of the THF solution); *cis*-$[(C_2H_5)_4N][Ta(CO)_4C_6H_5P\{CH_2CH_2P(C_6H_5)_2\}_2]$ (irradiation time 1 h; yield 75%; red oil after precipitation with pentane, solidifies on drying in vacuo); *cis*-$[(C_2H_5)_4N][Ta(CO)_4\{(C_6H_5)_2PCH_2CH_2P(C_6H_5)CH_2\}_2]$ (irradiation time 1.7 h; yield 73%; red powder, some of which precipitates out during concentration of the THF solution and more on addition of pentane). For $[Et_4N][Ta(CO)_4P_2]$ see also ref. 12.

$[Ta(H)(CO)_3P\{CH_2CH_2P(C_6H_5)_2\}_3]$: A solution of 630 mg (0.56 mmol) of $[Et_4N][Ta(CO)_4PP_3]$ in 10 ml of THF was injected onto a 6 cm diameter column filled with an 8 cm layer of a silica gel slurry and eluted with ca. 150 ml of THF. The yellow-orange fraction containing the hydrido complex was eluted (elution time 20 to 30 min; carbon monoxide is evolved during the elution). (A red fraction was subsequently eluted with acetonitrile, and shown to contain $[Et_4N][Ta(CO)_6]$ as the main product.) The THF solution of the hydrido complex was concentrated (vacuum, room temperature) to 15 ml, and dropwise addition of 30 ml of n-pentane produced an orange-red powder which was filtered off, washed with 5 ml of pentane, and dried under high vacuum for 4 h. Yield: 410 mg (0.44 mmol) = 79%.

The tetracarbonylhydrido complex with P_2 and the tricarbonylhydrido species with P_3 and P_4 were prepared analogously: *cis*-$[Ta(H)(CO)_4(C_6H_5)_2PCH_2CH_2P(C_6H_5)_2]$ (1.34 mmol $[Et_4N][Ta(CO)_4P_2]$ dissolved in 15 ml THF/MeCN 3/1; red powder; yield 84%); $Ta(H)(CO)_3C_6H_5P\{CH_2CH_2P(C_6H_5)_2\}_2]$ (0.54 mmol dissolved in 10 ml THF/MeCN 3/1; orange-red powder; yield 80%); $[Ta(H)(CO)_3\{(C_6H_5)_2PCH_2CH_2P(C_6H_5)CH_2\}_2]$ (0.73 mmol dissolved in 10 ml THF; red powder; yield 70%). In the case of P_3 and P_4, the products initially coming off the column are mainly $HTa(CO)_4P_m$ (see Table 1 and Fig. 1 for the IR characterization). The THF solutions of these tetracarbonyl species are transformed to $HTa(CO)_3P_m$ within a few hours at room temperature or after some days at 258 K).

trans-[Ta(H)(CO)₂{(C₆H₅)₂PCH₂CH₂P(C₆H₅)₂}₂]: A solution of 750 mg (1.09 mmol) of $HTa(CO)_4P_2$ in 100 ml of THF was irradiated for 30 min. White and light-red decomposition products were removed by filtration and the filtrate was evaporated to dryness to yield a red-orange powder of the hydrido complex, which was dried under high vacuum for 4 h. Yield: 520 mg (0.5 mmol) 46% based on $HTa(CO)_4P_2$ taken.

Acknowledgement

This work was supported by the Deutsche Forschungsgemeinschaft and the Fonds der Chemischen Industrie.

References

1 U. Franke and E. Weiss, J. Organomet. Chem., 152 (1978) C19.
2 D. Wenke and D. Rehder, J. Organomet. Chem., 273 (1984) C43.
3 J.E. Ellis and R.A. Faltynek, J. Organomet. Chem., 93 (1975) 205.
4 K. Ihmels and D. Rehder, J. Organomet. Chem., 218 (1981) C54.
5 J.E. Ellis, R.A. Faltynek, G.L. Rockfort, R.E. Stevens and G.A. Zank, Inorg. Chem., 19 (1980) 1082.
6 A. Davison and J.E. Ellis, J. Organomet. Chem., 36 (1972) 131.
7 D. Rehder, P. Oltmanns, M. Hoch, C. Weidemann and W. Priebsch, J. Organomet. Chem., 308 (1986) 19.
8 F. Calderazzo, G. Pampaloni and P.F. Zanazzi, Chem. Ber., 119 (1986) 2796.
9 K. Ihmels and D. Rehder, Organometallics, 4 (1985) 1334.
10 U. Puttfarcken and D. Rehder, (a) J. Organomet. Chem., 185 (1980) 219; (b) Z. Naturforsch. B, 37 (1982) 348; (c) J. Organomet. Chem., 184 (1980) 343.
11 K. Bachmann and D. Rehder, J. Organomet. Chem., 276 (1984) 177.
12 A. Davison and J.E. Ellis, J. Organomet. Chem., 31 (1971) 239.
13 P. Meakin, L.J. Guggenberger, F.N. Tebbe and J.P. Jerson, Inorg. Chem., 13 (1974) 1025.
14 U. Putterfarcken and D. Rehder, J. Organomet. Chem., 157 (1978) 321.
15 S. Datta, B. Dezube, J.K. Kouba and S.S. Wreford, J. Am. Chem. Soc., 100 (1978) 4404.
16 F.N. Tebbe, J. Am. Chem. Soc., 95 (1973) 5823.
17 T. Greiser, U. Puttfarcken and D. Rehder, Trans. Met. Chem., 4 (1979) 168.
18 F. Calderazzo, U. Englert, G. Pampaloni, G. Pelizzi and R. Zamboni, Inorg. Chem., 22 (1983) 1865.